

Overdensities Of Extremely Red Objects In The Fields Of High-Redshift Radio-Loud Quasars

M. Wold¹ and L. Armus

SIRTF Science Center, California Institute of Technology, MS 100-22, Pasadena, CA-91125

G. Neugebauer

California Institute of Technology, MS 105-24, Pasadena, CA-91125

T. H. Jarrett

IPAC, California Institute of Technology, MS 100-22, Pasadena, CA-91125

M. D. Lehnert

Max Planck Institute for Extraterrestrial Physics, Giessenbachstraße, 857488, Garching

ABSTRACT

We have examined the occurrence of Extremely Red Objects (EROs) in the fields of 13 luminous quasars (11 radio-loud and two radio-quiet) at $1.8 < z < 3.0$. The average surface density of $K_s \leq 19$ mag EROs is two-three times higher than in large, random-field surveys, and the excess is significant at the $\approx 3\sigma$ level even after taking into account that the ERO distribution is highly inhomogeneous. This is the first systematic investigation of the surface density of EROs in the fields of radio-loud quasars above $z \approx 2$, and shows that a large number of the fields contain clumps of EROs, similar to what is seen only in the densest areas in random-field surveys. The high surface densities and angular distribution of EROs suggest that the excess originates in high-redshift galaxy concentrations, possibly young clusters of galaxies. The fainter EROs at $K_s \gtrsim 19$ mag show some evidence of being more clustered in the immediate 20 arcsec region around the quasars, suggesting an association with the quasars. Comparing with predictions from spectral synthesis models, we find that if the $K_s \approx 19$ mag ERO excess is associated with the quasars at $z \approx 2$, their magnitudes are typical of $\gtrsim L^*$ passively evolving galaxies formed at $z \approx 3.5$ ($\Omega_m = 0.3$, $\Omega_\Lambda = 0.7$, and $H_0 = 70 \text{ km s}^{-1} \text{ Mpc}^{-1}$). Another interpretation of our results is that the excess originates in concentrations of galaxies at $z \approx 1$ lying along the line of sight to the quasars. If this is the case, the EROs may be tracing massive structures responsible for a magnification bias of the quasars.

Subject headings: galaxies:high-redshift—galaxies:clusters—galaxies: quasars—infrared:galaxies

1. Introduction

The age and space density of the oldest and most massive galaxies at each epoch provide the strongest constraints on models of galaxy formation. This is one of main reasons that there has been so much focus on Extremely Red Objects (EROs). It is the high-redshift systems that are most important for testing models, and the ERO selection criterion is designed to find old, passively evolving galaxies at $z \gtrsim 1$. Because the 4000 Å break in evolved galaxies shifts from optical to near-infrared at $z \gtrsim 1$, EROs are defined in terms of optical to near-infrared color, with two of the most used definitions being $R - K \geq 5.0$ and $I - K \geq 4.0$ mag.

The co-moving volume density, or even the number density, of massive, evolved galaxies at $z \gtrsim 1$ can place strong constraints on models of galaxy formation. Whereas monolithic collapse models (Eggen, Lynden-Bell, & Sandage 1962; Larson 1974; Tinsley & Gunn 1976; Loeb & Peebles 2003) predict pure luminosity evolution of early-type galaxies from the period of formation until the present-day, hierarchical formation models (White & Rees 1978; Baugh, Cole, & Frenk 1996; Kauffmann 1996; Baugh et al. 1998; Somerville, Primack, & Faber 2001) predict significant density evolution from $z \approx 1$ to $z \approx 0$. Testing the models has proven to be difficult, and the results are not yet conclusive. Some surveys have found a deficit of early-type galaxies at $z \approx 1$ (Barger et al. 1999; Smith et al. 2002; Roche et al. 2002) whereas others have not (Daddi, Cimatti, & Renzini 2000b; Cimatti et al. 2002; Im et al. 2002). Part of the disagreement may be caused by the strong clustering of EROs on the sky (Daddi et al. 2000a; Firth et al. 2002; Roche et al. 2002), and large fields must be surveyed in order to overcome this problem.

The ERO definition also selects dusty starburst galaxies whose spectral energy distribution can mimic those of old, passively evolving galaxies. It is still unclear how large a fraction of the ERO population consists of dusty starburst galaxies. Several methods are being used to separate the two galaxy types, including photometric (Mannucci et al. 2002; Smail et al. 2002; Miyazaki et al. 2002), spectroscopic (Cimatti et al. 2002; Saracco et al. 2003), and those based on morphology (Moriondo, Cimatti, & Daddi 2002; Stiavelli & Treu 2000; Yan & Thompson 2003). The results so far seem to suggest that roughly two-thirds of the EROs at $K \leq 19$ mag are old, passively evolving galaxies. However, it is also clear that the situation is more complex than just a simple distinction into old, evolved galaxies and dusty starbursts since systems with old populations and residual star formation also appear in ERO samples (Yan & Thompson 2003).

In this paper, we are concerned with EROs in the fields of high-redshift quasars. Some early studies serendipitously found EROs in the fields of $z > 2$ radio galaxies and quasars (McCarthy, Persson, & West 1992; Hu & Ridgway 1994; Dey, Spinrad, & Dickinson 1995). Although some of these EROs were later shown to lie in the foreground of the radio galaxies (Graham & Dey 1996), probing the fields around high-redshift radio-loud AGN (active galactic nuclei) has been a promising method of finding high-redshift galaxies. Luminous quasars and radio galaxies are often associated with high-density galaxy environments (Ellingson, Yee, & Green 1991; Hill & Lilly 1991; Hall & Green 1998; Wold et al. 2000; Best 2000; Venemans et al. 2002; Best et al. 2003), and the rich environments are often interpreted as clusters or groups of galaxies hosting the AGN. By combining a targeted search with a color criterion like that of EROs, high-redshift early-type

¹JPL Postdoctoral Researcher

galaxies can be effectively filtered out from the numerous foreground galaxies. This becomes very important at high redshifts, since even for a rich cluster at $z \approx 1$, most of the galaxies observed using a single broad-band filter are foreground or background galaxies (Dickinson 1997). A few surveys have found that EROs seem to be more common in high-redshift AGN fields than in the general field (Chapman, McCarthy, & Persson 2000; Cimatti et al. 2000; Hall et al. 2001; Sánchez & González-Serrano 2002), and there are individual AGN fields which show striking overdensities of EROs (Thompson, Aftreth, & Soifer 2000; Liu et al. 2000; Haines et al. 2001).

Even though galaxy excess in the fields of AGN are often being interpreted as groups or clusters physically associated with the AGN (spectroscopically confirmed in a few cases (Dickinson 1997; Deltorn et al. 1997)), gravitational lensing is also known to cause correlations (and anti-correlations) between high-redshift quasars and optically bright foreground galaxies (Webster et al. 1988; Hammer & LeFèvre 1990; Benítez, Martínez-González, & González-Serrano 1995; Benítez, Martínez-González, & Martín-Mirones 1997; Norman & Impey 2000; Myers et al. 2003). It is possible that a similar situation could arise between high-redshift quasars ($z \gtrsim 2$) and EROs, because the EROs are likely to be tracers of massive structures which may boost the fluxes of distant background quasars by gravitational lensing.

The aim with our present study is to test whether EROs are more common in the fields of $z \gtrsim 2$ quasars. To our knowledge, this is the first systematic survey to probe the surface density of EROs in the fields of quasars at $z > 2$, and preliminary results were reported by Wold et al. (2003). The quasars in our sample are selected from the catalogs of Barthel et al. (1988) and Hewitt & Burbidge (1993), and

form a subset of a larger sample of 40 designed to study host galaxies (Armus et al. in preparation). The 40 sample quasars are nearly evenly divided between radio-loud and radio-quiet systems with comparable V magnitudes and redshifts. The subsample of 13 analyzed here were selected randomly from the sample of 40 and followed up with wide-field near-infrared and optical imaging. The sample is listed in Table 1. In this table, we have also listed the radio loudness, defined in terms of the ratio of the flux densities at rest-frame 5 GHz and 2500 Å, S_{5GHz}/S_{2500} (Sramek & Weedman 1980). According to the definition by Kellermann et al. (1989), a quasar is radio-loud if $S_{5GHz}/S_{2500} > 10$, and thus two of the 13 quasars are classified as radio-quiet (one of these might be radio-intermediate instead of radio-quiet) whereas the rest are radio-loud. In calculating the radio loudness, we used the K_s -band fluxes of the quasars as found from our data, and the radio fluxes at 5 GHz listed in the catalog of Barthel et al. (1988) unless otherwise is noted in the table. The K_s -band fluxes were converted to rest-frame 2500 Å by assuming a power-law spectrum, $S_\nu \propto \nu^{-\alpha}$, where α was found from the median quasar energy distribution by Elvis et al. (1994). The conversion to rest-frame 5 GHz radio flux was done by assuming the same power-law form of the spectrum, but using spectral indices listed in the catalog by Barthel et al. (1988), unless otherwise is noted in the table.

The structure of the paper is as follows. In the next section, we describe the observations and data reduction. Section 3 deals with the construction of object catalogs and addresses their incompleteness. In Section 4 we present the results of the analysis. The surface density of EROs is calculated and the ERO excess evaluated, carefully taking into account their strong clustering. We also investigate the K_s -band number counts and the radial distribution of EROs around the quasars. In

TABLE 1
THE QUASAR SAMPLE.

Quasar (1)	$\frac{S_{5\text{GHz}}}{S_{2500}}$ (2)	z (3)	R (4)	K_s (5)
0741+169	3880 ^a	1.894	7500	3280
0758+120	1690	2.660	3600	2360
0830+115	2050	2.974	4550	2720
0927+217	130	1.830	3600	3280
0941+261	5750	2.910	2400	2240
1056+015	<14 ^b	2.650	11100	3260
1354+258	1080	2.032	2500	6800
1456+092	2590	1.991	3900	3200
1629+680	4070	2.475	6100	3780
1630+374	<6 ^b	2.037	3600	2920
1702+298	18130	1.927	4000	3340
2150+053	3330	1.979	2000	3040
2338+042	4915	2.594	3600	2880

NOTE.— (1) IAU designation. (2) Radio loudness defined as the ratio of the flux densities at rest-frame 5 GHz and 2500 Å (Sramek & Weedman 1980). (3) Redshift. (4)–(5) Total exposure time in seconds in the R - and K_s -filters.

^aRadio flux density and spectral index from the Green Bank radio survey by Becker, White, & Edwards (1991).

^bUpper limit based on a 3σ detection in the NRAO-VLA Sky Survey (Condon et al. 1998) and an assumed spectral index of $\alpha = 0.7$.

Section 5, we discuss two different interpretations of the results, and the conclusions are drawn in Section 6.

All magnitudes are given in the Vega system, and our assumed cosmology has $\Omega_m = 0.3$, $\Omega_\Lambda = 0.7$, and $H_0 = 70 \text{ km s}^{-1} \text{ Mpc}^{-1}$.

2. Observations and data reduction

The data consist of wide-field R - and K_s -band images taken with the Palomar 200-inch telescope using the prime-focus instruments COSMIC² (Kells et al. 1998) and PFIRCAM³ (Jarrett et al. 1994a). The COSMIC instrument is equipped with a 2048×2048 Tektronix CCD with a pixel scale of 0.2856 arcsec, and the PFIRCAM employs a 256×256 HgCdTe array with a pixel scale of 0.494 arcsec. The resulting fields of view in R and K_s are therefore 9.7×9.7 and 2.1×2.1 arcmin², respectively.

Images were obtained during several observing runs from September 1995 to July 2001. We used a 9- or 27-point dither pattern for the K_s images, and on-chip integration times of 4 sec. The number of co-adds was set so that the total integration time at each dither point was 20–30 sec, and the offsets between individual frames were typically 10–15 arcsec. The R -band exposures were divided into integrations of 300–600 sec each, with an offset of 10–20 arcsec between each exposure. The total integration time in R and K_s for each field is listed in Table 1.

Flat-field images in K_s were made by taking the median of dark-subtracted quasar images. Typically, a flat-field was made for each dither sequence, and this was found to be sufficient in most cases. After flat-fielding, the images were sky subtracted, corrected for bad pixels and registered using the DIMSUM pack-

age (Stanford, Eisenhardt & Dickinson 1995) within IRAF.⁴

The sky subtraction in DIMSUM is performed by subtracting a running sky frame made by taking the median of nine neighboring images. After the sky subtraction, masks are created for objects and cosmic rays and the masks are utilized to make a first pass combined image. The first pass image is then used to make a new and improved mask by including fainter objects. The new object mask is used in the final pass where the sky subtraction is repeated and the images aligned and combined. At this final step, we block replicated the images by a factor of two so that sub-pixel shifts were used for the aligning. The resulting images therefore have a pixel scale of 0.247 arcsec.

The R -band images were reduced in IRAF in a standard manner. The bias level was subtracted either by using a bias frame or by using a 3rd order Legendre to fit the overscan region which was then subtracted from each row. A flat-field was formed for each quasar field by taking the median of the quasar images, or of the quasar images in combination with exposures of other fields taken near in time. Typically 15–30 frames were used for this, and all emission $\approx 2\sigma$ above the average background was masked out. This method rejected cosmic rays, stars and galaxies visible in the quasar images and yielded a high quality flat-field frame. The flat-fielded images were then aligned using 20–40 stars in each frame, and averaged using *imcombine* with a high threshold set to remove bad pixels that had been flagged by giving them high, discrepant values. The combined R images were aligned with, and put to the pixel scale of, the

²Carnegie Observatories Spectrograph and Multiple Imaging Camera

³Prime Focus Infrared Camera

⁴IRAF is distributed by the National Optical Astronomy Observatories, which are operated by the Association of Universities for Research in Astronomy, Inc., under cooperative agreement with the National Science Foundation.

K_s images using the IRAF tasks *geomap* and *geotran*.

The flux calibration of the R -band images was accomplished using standard stars from Landolt (1992), and the K_s -data were calibrated using standard stars from Persson et al. (1998). The conditions were photometric, and the transparency good throughout most of the runs. The final photometric status was checked by the amount of variation within the individual exposures of the same source and by following standard stars throughout the night. For fields that were imaged during non-photometric conditions, calibration images were obtained later during photometric conditions to allow for an accurate flux calibration. During the photometric nights, the zeropoint varied by less than 0.1 mag. For a subset of the images, we checked our absolute photometry against the Two Micron All Sky Survey (2MASS) point source catalog (Skrutskie et al. 1997; Cutri et al.⁵). A very good agreement, typically < 0.1 mag difference, was found between our K_s -magnitudes and the 2MASS K_s -magnitudes for bright stars of $K_s \lesssim 15$ mag.

The full width at half maximum (FWHM) of the seeing in the K_s -images is 0.8–1.0 arcsec, and in the R -images, typically 1.0–1.5 arcsec. The raw number counts of galaxies with detection significance $\geq 3\sigma$ turns over at $K_s \approx 20$ mag, although this varies somewhat from field to field due to the different exposure times. In the R -band the corresponding turn-over in the number counts is $R \approx 24.5$ mag. The 3σ detection limits in the images are $K_s \approx 21.5$ and $R \approx 26$ mag. We address the completeness of the images in the next section.

⁵<http://www.ipac.caltech.edu/2mass/releases/second/doc/explsup.html>

3. Construction of object catalogs

3.1. Source detection

For object detection and photometry we used the SEXTRACTOR software package (Bertin & Arnouts 1996). In order to have the same FWHM of the seeing in both R and K_s we convolved the K_s -band images with a Gaussian function using the IRAF task *gauss* prior to object detection. For each field, object catalogs were constructed based on the detections in the K_s -band image. During the detection process, we used a Gaussian convolution filter with a FWHM matched to the seeing and a detection threshold of 1.5σ . Since the images were block replicated, we set the minimum number of pixels above the threshold to 20 in order to avoid spurious detections and cosmic rays over an area of less than 5 pixels in the original images. The result of the detection process was inspected visually in order to ensure that no obvious objects were missed, and that no false detections were entered into the catalogs. Saturated objects and objects lying close to the image boundaries were rejected from the catalogs.

Because of the dithering technique used in the K_s -band, the exposure time falls off toward the edges in the final combined images. Since the PFIRCAM field of view is relatively small, we included lower exposure regions, but rejected the regions where the exposure time is less than 25 % of the total, i.e. where the signal-to-noise drops by more than 50 %. This causes the rms background noise to increase toward the edges, resulting in a number of spurious detections. In order to avoid such spurious detections, we used the exposure maps produced by DIMSUM as weights in SEXTRACTOR. This allows for an adjustment of the detection threshold according to the noise level.

After the K_s -catalogs were made, matched R -band catalogs were created by running SEX-

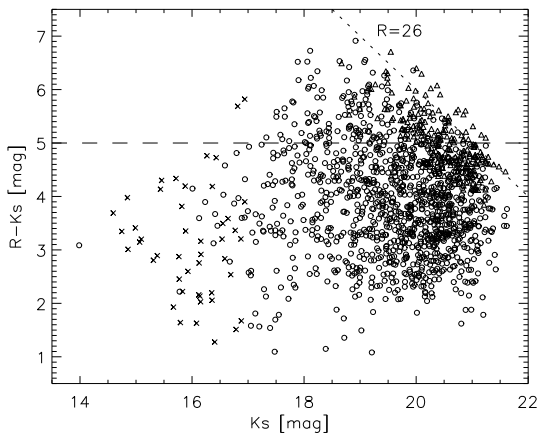


Fig. 1.— The circles show objects detected at a significance $\geq 5\sigma$ in the K_s -filter. The triangles are objects with a detection significance $< 3\sigma$ in the R -filter where a lower limit to the $R - K_s$ color has been calculated assuming a 3σ detection in R . The crosses are objects classified as stars. The horizontal line indicates our ERO definition, and the diagonal line the $R = 26$ mag limit. The scatter of objects above the diagonal line arises from the varying depths of the R -band images.

TRACTOR in double image mode. This produces a catalog of fluxes measured in the R -band image, but using the K_s -band image for detection. For total magnitudes, we used the SEXTRACTOR *best* magnitudes which are evaluated using adaptive apertures, or using isophotal corrections if a neighbor is suspected of biasing the adaptive aperture magnitude (Bertin & Arnouts 1996). For determining colors, we used aperture magnitudes, and chose an aperture diameter of two times the FWHM of the seeing, corresponding to typically 9–10 pixels, or 2.2–2.5 arcsec.

For each K_s -selected object, we calculated the detection significance using the uncertainty in the flux as measured by SEXTRACTOR which takes into account the Poissonian nature of the counts and the standard deviation in the background counts. In addition to this, we added in quadrature the error arising from the fluctuating background level across the image (Best 2000). In order for a K_s -selected object to be included in the catalog we required the detection significance within the aperture to be $\geq 5\sigma$. If the flux measured within the corresponding aperture in the R -band was significant at the $\geq 3\sigma$ level, we evaluated the $R - K_s$ color, and if $< 3\sigma$, a lower limit to the $R - K_s$ color was calculated assuming a 3σ detection in R .

In order to separate stars and galaxies, we used the star-galaxy classifier in SEXTRACTOR which assigns a probability between 0 and 1 to an object according to how likely it is to be a star. The star-galaxy classifier works well, but becomes less reliable at faint magnitudes. We therefore performed star-galaxy separation only at $K_s \leq 17$ mag, rejecting objects with a star-galaxy class of ≥ 0.85 from the catalogs. The star-galaxy separation was based on the detections in the K_s images.

3.2. Completeness

To be able to address the completeness of the K_s -band catalogs, we added artificial galaxies to the images using the IRAF task *mkobjects*. For a given input magnitude, we added galaxies with both deVaucouleurs and exponential disk profiles, in total ≈ 1500 galaxies distributed over the 13 fields. The scale-lengths of the artificial galaxies were randomly selected from the FWHM of the objects in the catalogs, and the images convolved with the same Gaussian function as was used to put the K_s -band images to the seeing of the R -band images. After this, the images were processed through SEXTRACTOR using the same detection criteria as described above.

The simulations show that for input objects of $K_s = 18$ mag, 96 % of the galaxies are recovered, where the missing 4 % is due to blending with other objects. At $K_s = 19$ mag the completeness drops to 90 %, and at $K_s = 20$ mag the catalogs are ≈ 40 % complete. The numbers were evaluated assuming a 50:50 mix of deVaucouleurs and exponential disk profiles.

4. Results

4.1. The surface density of EROs

We select EROs in the quasar fields using the criterion $R - K_s \geq 5.0$ mag. This includes old, passively evolving galaxies at $z \geq 0.9$, but also dusty starbursting galaxies. With only two filters, and at the resolution of our images, it is not possible to distinguish between these two galaxy types. There will also be some contamination by faint, red stars in our ERO sample as discussed below. We have chosen the $R - K_s \geq 5.0$ mag selection criterion because of two reasons. Firstly, because selecting galaxies with red colors enables us to eliminate a large part of the numerous foreground galaxies at $z < 1$ while at the same

time producing a big enough sample to perform meaningful statistics on. Secondly, because several random-field surveys employing the $R - K_s \geq 5.0$ mag criterion exist with which we can compare the ERO surface density. Our areal coverage in R and K_s is limited by the small field of view of the PFIRCAM instrument, so the field counts cannot be estimated from the quasar images themselves.

The color-magnitude diagram of all the K_s -selected objects is shown in Fig. 1. Above our $R - K_s \geq 5.0$ mag selection there are 253 objects, and 105 of these have a detection significance in R of three or less, i.e. the lower limit on their $R - K_s$ color is ≥ 5.0 mag. The SEXTRACTOR star-galaxy classifier finds that two of the EROs at $K_s \leq 17$ mag are stars, and these are excluded from the ERO sample, resulting in a total of 251 galaxies (including the $\leq 3\sigma$ detections in R having a lower limit of $R - K_s \geq 5.0$ mag).

In Fig. 2, we have plotted the average cumulative surface density of EROs in the quasar fields together with ERO surface densities found in the random-field surveys of Daddi et al. (2000a), Scodreggio & Silva (2000), Cimatti et al. (2002), Roche et al. (2002), and Miyazaki et al. (2002). Note that we have not compared with field counts derived from other colors (e.g. $I - K$ or $I - H$) since they may bias toward later-type galaxies with prolonged star formation (McCarthy et al. 2001; Yan & Thompson 2003). Note also that Miyazaki et al. define EROs as having $R - K_s(AB) \geq 3.35$ mag, which, according to Miyazaki et al., corresponds to $R - K_s(Vega) \geq 4.95$ mag.

The literature surveys cover wide, random areas and should therefore be representative of the ERO counts in the general field. The field counts agree well with each other except for the counts in the Chandra Deep Field South by Scodreggio & Silva (2000), which are consistently lower than the other. This is

most likely caused by the inhomogeneity of the ERO distribution coupled with the relatively small (and contiguous) area surveyed by Scodreggio & Silva. Fig. 2 demonstrates that the ERO counts in our quasar fields are systematically higher than those in the field. At $K_s \leq 19$ mag, where our counts are complete, the average surface density of EROs is two–three times larger than the average of the field values (excluding those in the Chandra Deep Field South). According to the average of the random-field surveys, as indicated by the dotted line in Fig. 2, we expect 34 ± 14 EROs at $K_s \leq 19$ mag over an area equal to the total area of our survey. (The error in this number takes into account the strong clustering of EROs as explained below.) The observed number of EROs in the quasar fields at $K \leq 19$ mag is 79, hence there is a significant excess above the field counts. At $K_s \gtrsim 20$ mag we still see a clear excess in the quasar fields, but our counts become strongly affected by incompleteness.

The number of EROs per quasar field and the average cumulative surface density as a function of K_s -magnitude is listed in Table 2. Some fields are seen to be very rich in EROs, such as 1456+092 and 2150+053, with surface densities four–five times larger than the field values. These fields have ERO excesses in every magnitude bin. Other fields have surface densities consistent with the field counts, like 0741+169 and 1629+680. The majority of the fields, however, have surface densities in between these two extremes. This is illustrated in Fig. 3, where a histogram of the ERO surface densities at $K_s \leq 19$ mag is shown. If the quasar fields were random with respect to the ERO distribution, we would expect a normal distribution centered on ≈ 0.546 arcmin⁻², which is the average surface density in the general field. This is not seen, instead there is a tail toward high surface densities, with as many as four fields (30 per cent of

the sample) having a surface density larger than three times the field value, and seven fields where the surface density is twice the field value. The combination of the very rich and the moderately rich fields gives an overall surface density well above the average for the random-field surveys.

4.2. Contamination by red stars

Of the 13 quasars fields, 10 lie at high galactic latitudes $b > 35^\circ$, so the contamination by stars is likely to be small. Using a color-cut of $R - K_s \geq 5.0$ mag will eliminate most field stars because of their bluer color, but L- and M-type dwarfs will be red enough to make it into our ERO sample. Based on $R - K'$ and $J - K'$ colors, Mannucci et al. (2002) find that 9 % of their $K' \leq 20$ mag ERO sample (at $b = -23^\circ$) is likely to consist of stars.

In order to estimate the contamination by stars, we used the stellar distribution model developed by Jarrett (1992) (see also Jarrett, Dickman, & Herbst (1994)). The model is an extension of the Bahcall & Soneira (1980) optical star count model to the near-infrared, and its performance with respect to 2MASS near-infrared star counts is demonstrated by Cambr esy et al. (2002). For every quasar position, we used the model to predict the expected number of stars having $R - K_s \geq 5.0$ mag. The predicted average surface density of stars for the whole ERO sample is listed on the bottom line of Table 2. These numbers show that 40–50 % of the brighter EROs at $K_s \leq 18$ mag might be stars, but that at fainter magnitudes the contamination decreases to 15–20 %. Note that this is an overestimate because the ERO counts suffer from incompleteness at fainter magnitudes. The 9 % contamination estimated by Mannucci et al. (2002) based on two colors therefore seems to agree well with the model predictions. We thus expect roughly 10 % of our EROs to be red stars. Since we cannot use the small

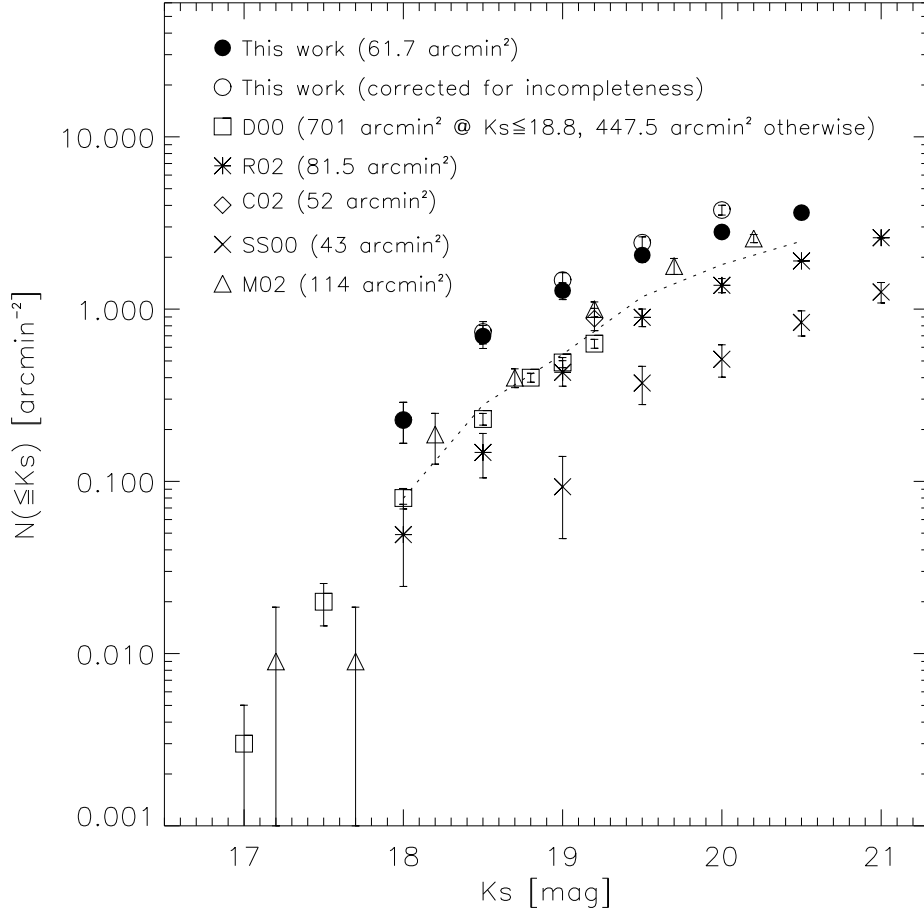


Fig. 2.— The cumulative surface density of EROs in the quasar fields compared with literature surveys in $R - K$ or $R - K_s$ covering wide, random fields (Roche et al. 2002 (R02); Cimatti et al. 2002 (C02); Miyazaki et al. 2002 (M02); Scodreggio & Silva 2000 (SS00); Daddi et al. 2000a (D00)). The average of the literature values (excluding the SS00 counts) is indicated by the dotted line. Error bars are Poissonian.

TABLE 2
THE CUMULATIVE NUMBER OF EROs IN THE QUASAR FIELDS AS A FUNCTION OF TOTAL K_s
MAGNITUDE.

Quasar	Area arcmin ²	≤ 18.0 mag	≤ 18.5 mag	≤ 19.0 mag	≤ 19.5 mag	≤ 20.0 mag	≤ 20.5 mag
0741+169	5.22	0	1	4	7	9	10
0758+120	5.23	2	5	6	8	12	16
0830+115	5.28	1	3	7	10	14	18
0927+217	4.19	1	4	8	12	18	22
0941+261	4.16	0	2	5	8	14	17
1056+015	5.13	0	2	4	6	8	16
1354+258	5.07	0	3	5	10	14	17
1456+092	4.34	2	4	10	12	15	19
1629+680	5.09	2	3	4	11	13	21
1630+374	4.30	1	2	2	5	5	5
1702+298	5.13	1	1	4	9	14	15
2150+053	4.21	2	7	10	13	16	21
2338+042	4.36	2	6	10	16	21	27
N_{qso}	61.7	14	43	79	127	173	224
n_{qso} (arcmin ⁻²)	...	0.23±0.06	0.70±0.11	1.28±0.14	2.06±0.18	2.80±0.21	3.63±0.25
n_{stars} (arcmin ⁻²)	...	0.11±0.04	0.17±0.05	0.25±0.06	0.44±0.08	0.47±0.09	0.59±0.10

NOTE.—The numbers in this table are based on raw counts. The bottom three lines show the total number of EROs in the 13 fields, N_{qso} , the resulting average surface density, n_{qso} , with its associated Poissonian error, and the expected surface density of stars, n_{stars} , with its associated Poissonian error. According to random-field surveys, the expected number of $K_s \leq 19$ mag EROs over 5 arcmin², the typical size of one quasar field, is two–three.

quasar fields for estimating the field counts of EROs, we compare the counts in the quasar fields with number densities of EROs from random-field surveys found in the literature. Since the random-field surveys are also contaminated by stars, a contamination of 10–20 % does not alter our conclusions.

The three lowest galactic latitude fields in our sample are 0741+169, 0758+120 and 0830+115 at $b = 20 - 27^\circ$. For these fields the model predicts 2.9, 2.6, and 1.6 stars at $K_s \leq 19$ mag, respectively. Note also that these are not among the richest fields in our sample.

4.3. Significance of the ERO excess

In this section we evaluate the significance of the ERO excess, taking into account the large variance in the ERO field counts caused by their strong clustering. The significance of the excess is given by

$$\sigma_{exc} = \frac{(N_{qso} - N_{field})}{\sigma} \quad (1)$$

(Yee & López-Cruz 1999), where N_{qso} is the total number of EROs in the quasar fields brighter than a given K_s -magnitude and N_{field} is the number of EROs in the random field scaled to the total area of the quasar fields, 61.7 arcmin². The error in the field counts expected over an area of 61.7 arcmin² is denoted σ . Ideally N_{field} should have been estimated from the edges of the quasar fields, but our fields are too small for this. Instead we use the average of the surface densities found by Daddi et al. (2000a), Roche et al. (2002), and Miyazaki et al. (2002).

Because ERO positions are correlated on the sky, the variance is given by

$$\sigma^2 = N_{field} (1 + N_{field} A_\omega C) \quad (2)$$

(Daddi et al. 2000a), where A_ω is the amplitude of the ERO angular two-point correlation function. The integral constraint which

arises from the fact that the survey area is limited is given by $A_\omega C$, and Daddi et al. find that C can be approximated by $58 \times Area^{-0.4}$. We use this approximation and find that $C = 11.15$ for the 13 quasar fields. The approximation is valid for a contiguous area, but serves our purpose well even if the 13 fields are non-contiguous. In any case, $C = 11.15$ is likely to be an overestimate since our fields are widely separated and not correlated in any way. We use the amplitudes, A_ω , found by Daddi et al. and Roche et al. for $K_s \leq 19$ mag and by Roche et al. for $K_s \leq 19.5$ mag, and calculate σ .

The result of the calculations for the entire quasar sample on average is shown in Table 3, where it can be seen that the excess at $K_s \leq 18$, 18.5 and 19 mag is significant at the $\approx 3\sigma$ level. Because of incompleteness, the excess is not significant at fainter K_s -levels, but if a correction is made for the incompleteness, the excess appears to be significant also at fainter K_s magnitudes, as shown in the last column of Table 3.

4.4. Radial distribution

If the EROs are associated with the quasars either through a surrounding cluster or a magnification bias we might expect to see a trend with projected quasar separation. In order to examine the radial distribution of EROs, we evaluated the average surface density in three annuli centered on the quasars, for three different magnitude intervals. The result is shown in Fig. 4. The brighter EROs at $17.5 \leq K_s < 19.5$ mag are seen to be uniformly distributed over the whole field, but the fainter ones at $K_s \gtrsim 19.5$ mag seem to cluster more in the immediate 20 arcsec region around the quasars. Note that this is not caused by the mosaicing technique in the K_s filter. The exposure times across the inner two annuli are uniform, with the third annulus being on the average only slightly less well ex-

TABLE 3
SIGNIFICANCE OF THE AVERAGE ERO EXCESS IN THE QUASAR FIELDS.

K_s	N_{qso}	$N_{field} \pm \sigma$	N_{exc}	σ_{exc}	σ_{exc}^{corr}
(1)	(2)	(3)	(4)	(5)	(6)
≤ 18.0	14	4.9 ± 3.4	9.1	2.7	...
≤ 18.5	43	17.2 ± 9.5	25.8	2.7	3.0
≤ 19.0	79	33.7 ± 14.3	45.3	3.2	4.0
≤ 19.5	127	72.8 ± 31.1	54.2	1.8	2.5
≤ 20.0	173	111.9 ± 34.4	61.1	1.8	3.5
≤ 20.5	224	153.1 ± 46.4	70.9	1.5	...

NOTE.—(1) K_s magnitude limit. (2) Total number of EROs in the 13 quasar fields. (3) The expected total number in the 13 fields based on the average of the literature counts, where σ is the uncertainty taking into account that the ERO distribution is inhomogeneous. (4) Excess above the field counts. (5)–(6) Significance of the ERO excess, calculated using Eq. 2. All numbers, except those in column (6), were evaluated using raw counts.

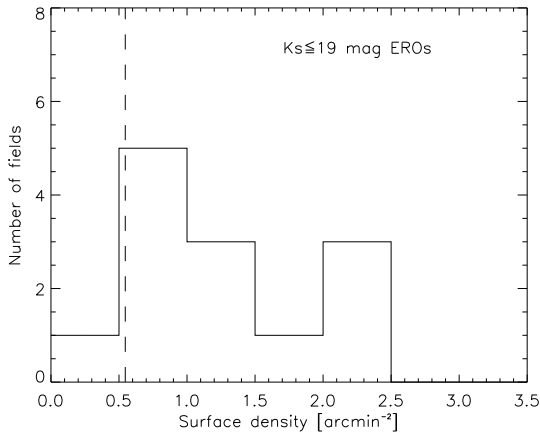


Fig. 3.— Histogram of raw ERO surface densities at $K_s \leq 19$ mag in the quasar fields. The vertical, dashed line indicates the average of the random-field surveys, $n = 0.546$ arcmin $^{-2}$.

posed than the other two. Using completeness simulations we find that the variation in the completeness level across the three annuli is at most a few per cent, i.e. consistent with what we expect from object crowding and blending. Therefore, there appears to be a real trend toward central concentration of the fainter EROs. Cimatti et al. (2000) looked for central concentrations of K_s -selected galaxies toward $z \approx 1.5$ radio-loud AGN. They did not find any significant trends, but noted that the regions closest to the AGNs had a higher number density of galaxies than in the general field.

4.5. The surface density of $R - K_s \geq 6.0$ mag EROs

For completeness, we also evaluated the surface density of $R - K_s \geq 6.0$ mag EROs. Using the redder color criterion gives a much smaller sample, 14 EROs at $K_s \leq 19$ mag

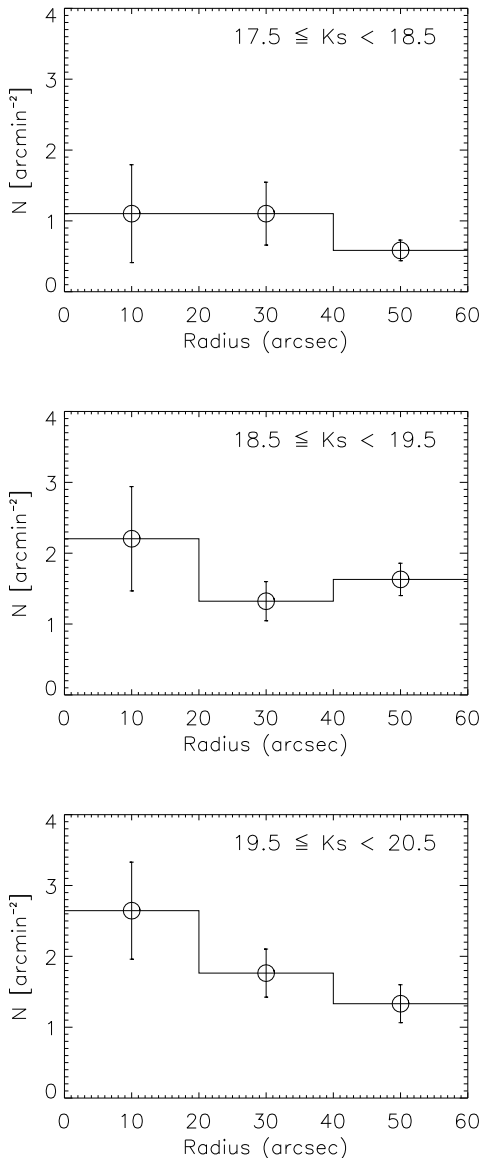


Fig. 4.— Mean radial distribution of EROs in the 13 quasar fields based on raw counts. The inner bin is centered on the quasars. The error bars show the standard deviation in the mean.

and 31 EROs at $K_s \leq 20$ mag. The resulting surface densities are thus 0.23 ± 0.06 and 0.50 ± 0.09 arcmin $^{-2}$ at $K_s \leq 19$ and ≤ 20 mag, respectively (Poissonian errors). The surface density of EROs at $K_s \leq 19$ mag is therefore 3–5 times higher than that found in the field surveys by Thompson et al. (1999) and Daddi et al. (2000a) (0.039 ± 0.016 and 0.07 ± 0.01 arcmin $^{-2}$, respectively). We also note that the surface density of $R - K_s \geq 6.0$ EROs in our quasar fields agrees with the ERO surface densities found in radio-loud AGN fields at $z = 1 - 1.5$ by Hall & Green (1998) and Cimatti et al. (2000).

4.6. K_s -band counts

Whereas there is a clear excess of EROs in the quasar fields, the overall K_s -counts show only a slight excess at fainter magnitudes, $K_s \gtrsim 18.5$ mag. This is seen in Fig. 5 where we have plotted the average K_s -band number counts together with counts from the surveys by Soifer et al. (1994), Moustakas et al. (1997), and Maihara et al. (2001), as well as the literature averages compiled by Hall, Green, & Cohen (1998) and Best et al. (2003). There are large field-to-field variations in the random-field K_s -band counts, and even though the counts in the quasar fields appear to lie above the literature averages at fainter K_s magnitudes, they are still consistent with the counts from the surveys by e.g. Soifer et al. (1994), Moustakas et al. (1997), and Maihara et al. (2001). We also find that the R -band number counts are consistent with the counts in the general field (Metcalf et al. 1995; Hogg et al. 1997). Overplotted in Fig. 5 are also the number counts of EROs in our fields, demonstrating, as expected, that non-ERO galaxies clearly dominate at all magnitudes.

Table 4 shows the fraction of EROs with respect to the whole K_s -selected sample of galaxies. For comparison, we have also listed

the ERO fractions given by Daddi et al. (2000a), Scodreggio & Silva (2000), and Roche et al. (2002), the latter calculated from their table 2. In the quasar fields, the EROs make up typically 20–25 % of all the K_s -selected galaxies, whereas the field surveys find $\lesssim 10$ %. We note that this behavior is what we expect if the EROs are tracing the early-type population in high-redshift clusters of galaxies since the fraction of early-type galaxies in rich clusters is known to be different from the field (Dressler 1980). This also illustrates the richness of EROs in the quasar fields, and suggests that the EROs are efficiently tracing overdensities not readily apparent from the K_s number counts alone. Clearly, the color-selection is very effective in eliminating foreground contamination.

5. Discussion

We have demonstrated above that the quasar fields have a significant excess of EROs above what is expected from the general field population of EROs, taking into account their strong clustering. It appears that the quasar fields contain clusters or dense concentrations of red galaxies, and their radial distribution suggests that the fainter EROs may be related to the quasars. However, another possibility is that the EROs are related to structures in the foreground of the quasars. We discuss each of these possibilities below. Note that our sample is dominated by radio-loud quasars, and that we restrict the following discussion to radio-loud quasars only.

5.1. ‘Clusters’ of EROs associated with the quasars

An argument in favor of the ERO excess being at the quasar redshifts is that luminous radio-loud quasars and radio galaxies at $z \lesssim 1$ are known to reside in regions of enhanced galaxy density, interpreted as clus-

ters or groups of galaxies physically associated with the AGN (Hall & Green 1998; Best 2000). Since powerful AGN with supermassive black holes may trace the densest regions, it is natural to assume that this is true also at $z \gtrsim 2$. For example, Cimatti et al. (2000) find excess EROs in radio-loud AGN fields at $z \approx 1.5$ and Best et al. (2003) find that red galaxies cluster around powerful radio sources at $z \approx 1.5$. Our study pushes this out to $z \gtrsim 2$.

If the ERO excess originates in dense environments associated with the quasars, the majority of the EROs must lie at $z \approx 2$ since this is the redshift of most of the quasars in our sample. It is therefore appropriate to discuss whether the color and the brightness of the EROs are consistent with being evolved galaxies at $z \approx 2$. We have used the PÉGASE models of Fioc & Rocca-Volmerange (1997) to examine both the apparent magnitude and the $R - K_s$ color of passively evolving galaxies at $z \approx 2$ (assuming no extinction by dust, and an initial metallicity of 1 % solar value). The apparent K_s magnitude of L^* galaxies at $z = 2$ was found by calculating the scale factor between the observed flux of the model and that of a present-day L^* galaxy. The present-day L^* galaxy was assumed to have $M_B^* = -20.3$ mag (Loveday et al. 1992) and an age of 14 Gyr.

The standard model in which the stars form in a 1 Gyr long burst at $z > 4$ has an $R - K_s$ color at $z = 2$ which is too red for most of our EROs. In order for this model to produce a color of $R - K_s = 5 - 6$ mag at $z = 2$, the formation redshift has to be $z \approx 3.5$. The K_s^* magnitude of such a galaxy observed at $z = 2$ is 19.2 mag. Since the star formation in this model stops abruptly after 1 Gyr, this model represents the galaxy which reddens most quickly. Therefore, $K_s = 19.2$ mag is the brightest magnitude we can expect for an L^* galaxy at $z = 2$. If the $K_s \approx 19$

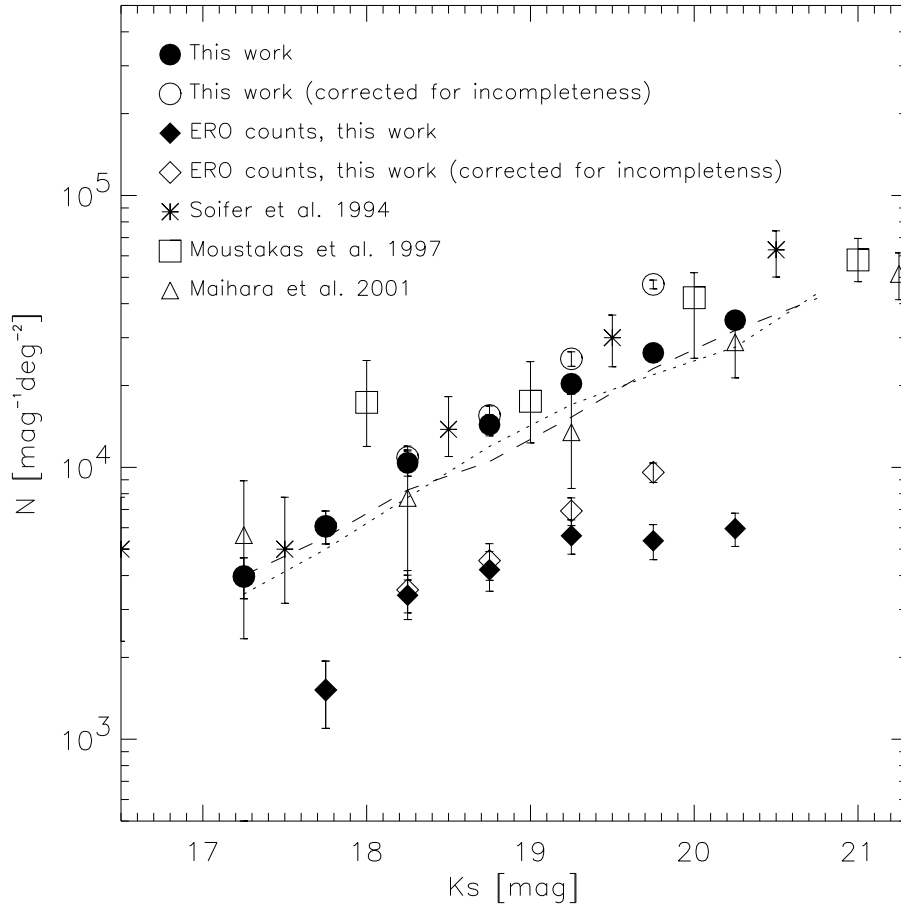


Fig. 5.— Number counts of K_s -selected galaxies (circles) and EROs (diamonds) detected at a significance greater than 5. We have compared with a selection of deep K -band surveys from the literature as shown by the other symbols. The dotted and dashed lines show the literature averages compiled by Hall, Green, & Cohen (1998) and Best et al. (2003), respectively.

TABLE 4
ERO FRACTIONS AMONG K_s -SELECTED GALAXIES.

K_s	This work	D00	SS00	R02
(1)	(2)	(3)	(4)	(5)
≤ 18.0	0.14 ± 0.04	0.05
≤ 18.5	0.22 ± 0.04	0.08
≤ 19.0	0.25 ± 0.03	0.12	0.02 ± 0.01	...
≤ 19.5	0.26 ± 0.03	...	0.06 ± 0.02	0.12 ± 0.02
≤ 20.0	0.24 ± 0.02	...	0.06 ± 0.01	0.14 ± 0.01
≤ 20.5	0.22 ± 0.02

NOTE.—(1) Magnitude limit. (2) Fraction of EROs evaluated using raw counts. (3)–(5) ERO fractions found by Daddi et al. 2000a (D00), Scodreggio & Silva 2000 (SS00), and Roche et al. 2002 (R02). The uncertainties are Poissonian.

mag ERO excess is associated with passively evolving galaxies at $z \approx 2$, they must therefore be $\gtrsim L^*$ galaxies. Other models which have $R - K_s = 5 - 6$ mag at $z = 2$ include those with exponentially decreasing star formation rates. For instance, a galaxy formed at $z = 6$ with an exponentially decreasing star formation rate of $\tau = 0.5$ Gyr has $R - K_s = 5 - 6$ mag at $z = 2$, and $K_s^* = 19.6 - 19.7$ mag. If the EROs are described by this latter model, they must have small amounts of residual star formation in them.

The recent spectroscopic work of van Dokkum et al. (2003) has shown that red galaxies at $z > 2$ can be very bright. Five of their six galaxies were found to lie at $2.4 \leq z \leq 3.5$ and to have K_s -magnitudes in the range 19.2–19.9 mag. These galaxies were selected by the $J - K_s > 2.3$ mag criterion (Franx et al. 2003), whereas our galaxies are selected on the basis of having $R - K_s \geq 5.0$ mag. Both criteria are designed to find galaxies with evolved 4000 Å breaks, but at dif-

ferent redshifts. However, these two selection techniques will not necessarily sample the same type of galaxies since the different filters sample different rest-frame wavelength ranges. While the results of van Dokkum et al. prove that high-redshift red galaxies can be bright, their spectroscopic sample (six of eleven $J - K_s$ -selected galaxies) may be biased toward systems with ongoing star formation.

The average ERO fraction in our quasar fields is above 20 %, and for the four richest fields in our sample the fraction is as high as ≈ 50 %. This is what we expect if the fields contain clusters or concentrations of galaxies with an already existing relation between morphology and density (Dressler et al. 1997). This is also the suggestion from the work by Best et al. (2003) who find that red galaxies are concentrated toward $z \approx 1.5$ powerful radio sources.

Whereas the magnitudes and colors of the EROs are consistent with models of passively evolving galaxies, another possibility is that

they might be starbursting systems reddened by dust. Hence, an alternative explanation is that the quasars live in dense environments dominated by galaxies with enhanced star formation. In this case, the excess EROs may be dusty starburst galaxies, possibly the progenitors of massive ellipticals in a forming cluster. There are examples of fields around high-redshift radio-loud AGN with excesses of star-forming galaxies such as Ly-alpha emitters (Kurk et al. 2000; Pentericci et al. 2000; Venemans et al. 2002). Also, Ivison et al. (2000) find a concentration of submm sources in the field of the $z = 3.8$ radio galaxy 4C 41.17 raising the possibility that the EROs in this field are dusty starburst systems rather than passively evolving galaxies. This possibility is also discussed by Smail et al. (2003) for a luminous submm source in the field of the radio galaxy 53W002 at $z = 2.4$.

One might expect a correlation between the radio properties of the quasars and their ERO excesses if there is e.g. a relation between radio power and black hole mass (Wold et al. 2000; Laor 2000; Lacy et al. 2001). We have checked this for our sample, but do not find that the radio power correlates with the ERO excess.

5.2. EROs in foreground lensing structures

Little is known yet of the luminosity function of EROs. In the spectroscopic survey by Cimatti et al. (2002), which is 67 % complete at $K_s \leq 19.2$ mag, the $R - K_s \geq 5.0$ mag EROs are found to lie at $z = 0.7 - 1.5$. The redshift distribution derived by Miyazaki et al. (2002) based on photometric redshifts is in broad agreement with Cimatti et al.'s, but has a tail toward higher redshifts. If we assume that our ERO sample has a redshift distribution similar to that found by Cimatti et al. and Miyazaki et al., we have to explain why the ERO surface density in the quasar

fields is so significantly different from that in the large random-field surveys. We are sampling the ERO distribution with several small, but widely separated fields, and should therefore be minimally affected by cosmic variance. Instead, the opposite seems to be the case; the quasar fields sample the densest regions in the ERO distribution. A large number of the quasar fields contain clumps of EROs, similar to what is seen only in the densest areas in the large random-field surveys. If the EROs have a peak redshift of $z \approx 1.0$, they must therefore be clusters of galaxies, or overdensities in the ERO distribution, lying along the lines of sight to the quasars.

A biasing of quasar lines of sight with respect to $z \approx 1$ overdensities in the ERO distribution can be explained by gravitational lensing. If we assume that the overdensities in the quasar fields do not extend much beyond the edges of the fields their typical scale is ~ 1 arcmin, corresponding to 2–3 Einstein radii for galaxy clusters at $z \sim 1$. The most efficient lens redshift for a quasar at $z = 2$ is 0.5–0.6, but a magnification can still occur if the lens lies at $z \sim 0.8 - 1.0$.

The quasars in our sample are very luminous, eight of them have $M_V < -27.2$ mag ($H_0 = 50 \text{ km s}^{-1} \text{ Mpc}^{-1}$), and hence classify as highly luminous quasars. They therefore fulfill the three criteria for maximizing the probability of a magnification bias, i.e. they are distant, bright and have a steep number-magnitude slope (Claeskens & Surdej 2002, and references therein). If a magnification bias is the explanation for our results, we might expect that the fields around the most luminous quasars contain the highest overdensities of EROs, but our data do not show any significant correlations between quasar luminosity and ERO surface density to support this.

Furthermore, if the majority of the EROs are associated with overdensities along the

line of sight to the quasars, we might expect the spectra of the quasars in the richest fields to have strong (rest-frame equivalent width $\gtrsim 0.7 \text{ \AA}$) metal absorption line systems (Liu et al. 2000). We have found absorption line data for seven of the 13 quasars in our sample (Junkkarinen, Hewitt, & Burbidge 1991, 1992). Two of the four richest fields have such data; Q2150+053 show no strong metal absorption lines and Q2338+042 have CIV and FeII at $z_{abs} \approx 1.80$ (Barthel, Tytler, & Thomson 1990). Other quasars with metal absorption line systems in the foreground is Q0830+115 with FeII at $z_{abs} = 0.92$ and MgII at $z_{abs} = 0.80$ (Sargent, Steidel, & Boksenberg 1989), Q0941+261 with MgII systems at $z_{abs} = 0.71$ and $z_{abs} = 1.09$, and Q1354+258 with MgII at $z_{abs} = 0.86$ and some weaker FeII and MgII systems at $z_{abs} = 1.42$ (Barthel, Tytler, & Thomson 1990), but these quasars lie in fields with relatively few EROs compared to the richer fields. The data for Q0758+120 and Q1629+680 show no strong metal absorption line systems (Barthel, Tytler, & Thomson 1990). There is thus no clear trend of increasing number of absorption line systems with ERO richness. Also, the quasars in our sample were not selected on the basis of having strong or numerous absorption line systems.

6. Conclusions

On the average, the quasar fields studied here have a cumulative surface density of EROs at $K_s \leq 18$, 18.5 and 19 mag which is two-three times larger than what is found in the general field. The excess is significant at the $\approx 3\sigma$ level even after taking into account that the ERO distribution is strongly clustered. There is also an excess of EROs at fainter magnitudes, but at $K_s \approx 20$ mag our counts become strongly affected by incompleteness and a secure quantitative estimate of the excess for $K_s > 20$ mag is difficult.

However, by making a correction for the incompleteness, we find that the ERO excess at $K_s \leq 19.5$ and $K_s \leq 20$ mag may also be significant at the $\gtrsim 3\sigma$ level.

The quasar fields are small, typically $2.1 \times 2.1 \text{ arcmin}^2$ (limited by the near-infrared field of view), but widely separated, and therefore sample the ERO population with minimal influence from cosmic variance. The fact that the excess is statistically significant therefore suggests that the quasar fields probe the densest regions in the ERO distribution, implying that the fields around luminous, high-redshift quasars are on the average, overdense in EROs. There are two possible explanations for the observed overdensities. (1) The majority of the EROs may be associated with concentrations of galaxies at the quasar redshifts, or (2) the EROs lie in the foreground, along the line of sight to the quasars.

Based on both spectroscopic observations of $z > 2$ red galaxies (van Dokkum et al. 2003) and spectral synthesis models (Fioc & Rocca-Volmerange 1997), we argue that a redshift of $z \approx 2$ for the EROs is plausible. The $K_s \approx 19$ mag ERO excess may therefore be physically associated with the quasars, in which case their magnitudes and colors are consistent with $\gtrsim L^*$ passively evolving galaxies.

The EROs at $K_s \geq 19 - 19.5$ mag are more clustered in the immediate 20 arcsec region around the quasars, hence the radial distribution supports the explanation that the fainter EROs are physically associated with the quasars. Furthermore, the fraction of EROs among the K_s -selected galaxies in the quasar fields is unusually high, typically 20–25 %, in contrast to $\lesssim 10$ % which is found in random-field surveys (Daddi et al. 2000a; Scodreggio & Silva 2000; Roche et al. 2002). This is consistent with the ERO excess being associated with dense concentra-

tions of red, possibly evolved, galaxies. The high ERO fractions may therefore indicate that a morphology-density relation (Dressler et al. 1997) exists in the quasar fields. The candidate ERO clusters in the quasar fields may therefore represent the oldest and most evolved systems at $z \gtrsim 2$, and will be crucial for testing models of structure and galaxy formation. If the ERO excess is dominated by dusty starforming galaxies instead of passively evolving galaxies, the EROs might be the progenitors of massive ellipticals in a forming cluster associated with the quasars.

The second explanation, that the ERO excess lies in the foreground, is equally interesting because it implies that the lines of sight toward high-redshift, luminous quasars are biased toward overdensities in the ERO distribution. In this case, the ERO excess is most likely associated with clusters of galaxies at $z \approx 1$ giving rise to a magnification bias of the quasars. In this interpretation, we would be seeing candidate clusters with passively evolving galaxies at $z \approx 1$, a redshift where still only less than a handful of clusters are known. However, we see no trend of quasar brightness with ERO overdensity as might be expected in this interpretation. Also, there is no association of the numbers of absorption line systems with ERO richness for seven of the 13 quasars with absorption line data.

With the current data, it is not possible to tell whether the ERO excess is part of a small-scale overdensity centered on, or lying close to, the quasars, or if it is part of a larger structure that extends over a wider area. To address this issue, we have begun an imaging program using J - and K_s -filters at the Palomar 200-inch telescope over much larger fields. With these data we will be able to trace the ERO population around the $z \approx 2$ quasars on scales up to 4–5 Mpc.

We are grateful to Dave Thompson, Lin

Yan and Mark Lacy for helpful discussions, and to the referee for a careful review of the manuscript. This publication makes use of data products from the Two Micron All Sky Survey, which is a joint project of the University of Massachusetts and the Infrared Processing and Analysis Center/California Institute of Technology, funded by the National Aeronautics and Space Administration and the National Science Foundation. This research has also made use of the NASA/IPAC Extragalactic Database (NED) which is operated by the Jet Propulsion Laboratory, California Institute of Technology, under contract with the National Aeronautics and Space Administration.

REFERENCES

- Bahcall, J. N., Soneira, R. M. 1980, *ApJS*, 44, 73
- Barger, A. J., Cowie, L. L., Trentham, N., Fulton, E., Hu, E. M., Songaila, A., & Hall, D., 1999, *AJ*, 117, 102
- Barthel, P. D., Tytler, D. R., & Thomson, B., 1990, *A&AS*, 82, 339
- Barthel, P. D., Miley, G. K., Schilizzi, R. T., & Lonsdale, C. J., 1988, *A&AS*, 73, 515
- Baugh, C. M., Cole, S., & Frenk, C. S., 1996, *MNRAS*, 283, 1361
- Baugh, C. M., Cole, S., Frenk, C. S., & Lacey, C. G., 1998, *ApJ*, 498, 504
- Becker, R. H., White, R. L., & Edwards, A. L., 1991, *ApJS*, 75, 1
- Benítez, N., Martínez-González, E., & González-Serrano, J. I., 1995, *AJ*, 109, 935
- Benítez, N., Martínez-González, E., & Martín-Mirones, J. M., 1997, *A&A*, 321, L1
- Bertin, E., Arnouts, S., 1996, *A&AS*, 117, 393

- Best, P. N., 2000, MNRAS, 317, 720
- Best, P. N., Lehnert, M. D., Miley, G., & Röttgering, H., 2003, MNRAS, in press (astro-ph/0304035)
- Cambrésy, L., Beichman, C. A., Jarrett, T.H., Cutri, R.M., 2002, AJ, 123, 2559
- Chapman, S. C., McCarthy, P., & Persson, S. E., 2000, AJ, 120, 1612
- Cimatti, A., Villani, D., Pozzetti, L., & di Serego Alighieri, S., 2000, MNRAS, 318, 453
- Cimatti, A., et al., 2002, A&A, 381, L68
- Claeskens, J.-F., Surdej, J., 2002, A&A Rev, 10, 263
- Condon, J. J., Cotton, W. D., Greisen, E. W., Yin, Q. F., Perley, R. A., Taylor, G. B., & Broderick, J. J., 1998, AJ, 115, 1693
- Daddi, R., Cimatti, A., Pozzetti, L., Hoekstra, H., Röttgering, H. J. A., Renzini, A., Zamorani, G., & Mannucci, F., 2000a, A&A, 361, 535
- Daddi, E., & Cimatti, A., Renzini, A., 2000b, A&A, 362, L45
- Deltorn, J.-M., Le Fèvre, O., Crampton, D., & Dickinson, M., 1997, ApJ, 483, L21
- Dey, A., Spinrad, H., & Dickinson, M., 1995, ApJ, 440, 515
- Dickinson, M. 1997, in *The Early Universe with the VLT*, ed. J. Bergeron (Berlin: Springer-Verlag), 274
- Dressler, A., 1980, ApJ, 236, 351
- Dressler, A., et al., 1997, ApJ, 490, 577
- Eggen, O. J., Lynden-Bell, D., & Sandage, A. R., 1962, ApJ, 136, 748
- Ellingson, E., Yee, H. K. C., & Green, R. F., 1991, ApJ, 371, 49
- Elvis, M., Wilkes, B. J., McDowell, J. C., Green, R. F., Bechtold, J., Willner, S. P., Oey, M. S., Polonski, E., & Cutri, R., 1994, ApJS, 95, 1
- Fioc, M., Rocca-Volmerange, B., 1997, A&A, 326, 950
- Firth, A. E., et al., 2002, MNRAS, 332, 617
- Franx, M., et al., 2003, ApJ, 587, 79L
- Graham, J.R., Dey, A., 1996, ApJ, 471, 720
- Haines, C. P., Clowes, R. G., Campusano, L. E., & Adamson A. J., 2001, MNRAS, 323, 688
- Hall, P. B., Green, R. F., 1998, ApJ, 507, 558
- Hall, P. B., Green, R. F., & Cohen, M., 1998, ApJS, 119, 1
- Hall, P. B., et al., 2001, AJ, 121, 1840
- Hammer, F., LeFèvre, O., 1990, ApJ, 357, 38
- Hewitt, A., Burbidge, G., 1993, ApJS, 87, 451
- Hill, G. J., Lilly, S. J., 1991, ApJ, 367, 1
- Hogg, D. W., Pahre, M. A., McCarthy, J. K., Cohen, J. G., Blandford, R., Smail, I., & Soifer, B. T., 1997, MNRAS, 288, 404
- Hu, E. M., Ridgway, S. E., 1994, AJ, 107, 1303
- Im, M., et al., 2002, ApJ, 571, 136
- Iverson, R. J., Dunlop, J. S., Smail, I., Dey, A., Liu, M. C., Graham, J.R., 2002, ApJ, 542, 27
- Jarrett, T. H., *An optical study of the faint end of the stellar luminosity function*, Ph.D. thesis, Massachusetts Univ., Amherst.

- Jarrett, T. H., Beichman, T. H., Van Buren, D., Jorquera, C., & Bruce, C. 1994a, in the Proceedings of the UCLA Conference on Infrared Astronomy with Arrays, ed. I. S. McLeean (Dordrecht: Kluwer)
- Jarrett, T. H., Dickman, R. L., & Herbst, W., 1994b, *ApJ*, 424, 852
- Junkkarinen, V., Hewitt, A., & Burbidge, G., 1991, *ApJS*, 77, 203
- Junkkarinen, V., Hewitt, A., & Burbidge, G., 1992, *ApJS*, 81, 409
- Kauffmann, G., 1996, *MNRAS*, 281, 487
- Kellermann, K. I., Sramek, R., Schmidt, M., Shaffer, D. B., & Green R., 1989, *AJ*, 98, 1195
- Kells, W., Dressler, A., Sivaramakrishnan, A., Carr, D., Koch, E., Epps, H., Hilyard, D., & Pardeilhan, G., 1998, *PASP*, 110, 1487
- Kurk, J. D., et al., 2000, *A&A*, 358, L1
- Lacy, M., Laurent-Muehleisen, S. A., Ridgway, S. E., Becker, R., & White, R. L., 2001, *ApJ*, 551, L17
- Landolt, A. U. 1992, *AJ*, 104, 340
- Laor, A., 2000, *ApJ*, 543, L111
- Larson, R. B., 1974, *MNRAS*, 169, 229
- Liu, M. C., Dey, A., Graham, J. R., Bundy, K. A., Steidel, C. C., Adelberger, K., & Dickinson, M., 2000, *ApJ*, 119, 2556
- Loeb, A., Peebles, P. J. E., 2003, *ApJ*, in press (astro-ph/0211465)
- Loveday, J., Peterson, B. A., Efstathiou, G., & Maddox, S. J., 1992, *ApJ*, 390, 338
- Maihara, T., et al., 2001, *PASJ*, 53, 25
- Mannucci, F., et al., 2002, *MNRAS*, 329, L57
- McCarthy, P. J., Persson, S. E., & West, S. C., 1992, *ApJ*, 386, 52
- McCarthy, P. J., et al., 2001, *ApJ*, 560, L131
- Metcalfe, M., Shanks, T., Fong, R., & Roche, N., 1995, *MNRAS*, 273, 257
- Miyazaki, M., et al., 2002, astro-ph/0210509
- Moriondo, G., Cimatti, A., & Daddi, E., 2000, *A&A*, 364, 26
- Moustakas, L. A., Davis, M., Graham, R. J., Silk, J., Peterson, B. A., & Yoshii, Y., 1997, *ApJ*, 475, 445
- Myers, A. D., Outram, P. J., Shanks, T., Boyle, B. J., Croom, S. M., Loaring, N. S., Miller, L., & Smith, R. J., 2003, *MNRAS*, in press
- Norman, D. J., Impey, C. D., 2000, *AJ*, 121, 2392
- Pentericci, 2000, *A&A*, 361, L25
- Persson, S. E., Murphy, D. C., Krzeminski, W., Roth, M., & Rieke, M. J., 1998, *AJ*, 116, 2475
- Roche, N. D., Almaini, O., Dunlop, J., Ivison, R. J., & Willott, C. J., 2002, *MNRAS*, 337, 1282
- Sánchez, S. F., & González-Serrano, J. I., 2002, *A&A*, 396, 773
- Saracco, P., et al., 2003, *A&A*, 398, 127
- Sargent W. L. W., Steidel, C. C., & Boksenberg, A., 1989, *ApJS*, 69, 703
- Scodreggio, M., Silva, D. R., 2000, *A&A*, 359, 953
- Skrutskie, M. F. 1997, in *The Impact of Large Scale Near-IR Sky Surveys*, eds. F. Garzon et al. (Dordrecht: Kluwer), 25

- Smail, I., Owen, F. N., Morrison, G. E., Keel, W. C., Ivison, R. J., & Ledlow, M. J., 2002, *ApJ*, 581, 844
- Smail, I., Ivison, R. J., Gilbank, D. G., Dunlop, J. S., Keel, W. C., Motohara, K., Stevens, J.A., 2003, *ApJ*, 583, 551
- Smith, G. P., et al., 2002, *MNRAS*, 330, 1
- Soifer, B. T., et al., 1994, *ApJ*, 420, L1
- Somerville, R. S., Primack, J. R., & Faber, S. M., 2001, *MNRAS*, 320, 504
- Sramek, R. A., Weedman, D. W., 1980, *ApJ*, 283, 435
- Stanford, S. A., Eisenhardt, P. R. M., & Dickinson, M., 1995, *ApJ*, 450, 512
- Stiavelli, M., Treu, T. 2000, in *Galaxy Disks and Disk Galaxies*, ASP Conf. Ser. Vol. 230, ed. J. G. Funes, S. J. & E. R. Corsini (San Francisco: Astronomical Society of the Pacific), 603
- Thompson, D., Aftreth, O., & Soifer, B. T., 2000, *ApJ*, 120, 2331
- Thompson, D., et al., 1999, *ApJ*, 523, 100
- Tinsley, B. M., Gunn, J. E., 1976, *ApJ*, 203, 52
- van Dokkum, P. G., 2003, *ApJ*, 587, L83
- Venemans, B. P., et al., 2002, *ApJ*, 569, L11
- Webster, R. L., Hewett, P. C., Harding, M. E., & Wegner, G. A., 1988, *Nat.*, 336, 358
- White, S. D. M., Rees, M. J., 1978, *MNRAS*, 183, 341
- Wold, M., Armus, L., Neugebauer G., Jarrett, T. H., & Lehnert, M. D. 2003, to appear in *Radio Galaxies: Past, Present and Future*, *New Astronomy Reviews*, ed. M. Jarvis et al., (Amsterdam: Elsevier) (astro-ph/0303090)
- Wold, M., Lacy, M., Lilje, P. B., & Serjeant, S., 2000, *MNRAS*, 316, 267
- Yan, L., Thompson, D., 2003, *ApJ*, 586, 765
- Yee, H. K. C., & López-Cruz, O., 1999, *AJ*, 117, 1985